Japan Journal of Research

Original Article

Statistical Analysis of Ultraviolet Radiation in The Museum of L'almoina in Valencia (Spain)

Juan-Carlos Moreno[1], José Luis Baró[2], María-Antonia Serrano[3], Fernando-Juan García-Diego[1*]

[1]Department Applied Physics, Universitat Politècnica de València, Camino de Vera, s/n, 46022 Valencia, Spain
[2]Department of Architectural Composition, Universitat Politècnica de València, Camino de Vera, s/n, 46022 Valencia, Spain
[3]Biomaterials and Tissue Engineering, Universitat Politècnica de València, Camino de Vera, s/n, 46022 Valencia, Spain

Correspondence
Juan-Carlos Moreno
Department Applied Physics, Universitat Politècnica de València, Camino de Vera, s/n, 46022 Valencia, Spain
E-mail: jcmestev@fis.upv.es
Tel: +34-9638-77000 (ext. 75241)

Abstract

The present work is an analysis and statistical association of distributions of experimental values of ultraviolet radiation attenuation through the skylight of a museum in the city of Valencia (Spain). The distributions of values were made in summer and winter at different times. Statistical analysis was obtained to detect the clustering of the measurement distributions, and the statistical association was carried out using the Q or Yule index, which means a dependency function between this parameter and the structure of the museum building. The basis of the aforementioned statistical index is a contingency matrix whose elements are subject to change depending on the season of the year and the shape of the skylight.

- Received Date: 09 Dec 2022
- Accepted Date: 14 Dec 2022
- Publication Date: 02 Jan 2023

Introduction

Preventive conservation and maintenance of archaeological sites is a cultural, ethical and moral necessity. In fact, it is manifested in the requirements of the main international charters on the protection of archaeological heritage [1-4]. Protection against light radiation and ultraviolet rays (UV) is essential, it is one of the factors in the proper conservation of cultural assets [5].

It is well known that prolonged exposure to visible light (VIS) causes the discoloration of pigments, and UV involves a yellowing and progressive disintegration of certain materials. In addition, the infrared (IR) band produces heating of the surface of objects with the consequent thermal deterioration of the objects [6].

The subject of analysis is a museum built in 2006 in Valencia (Spain). It was built to preserve an archaeological site dating back to the founding of the city in the Roman Republican era [7, 8]. The site is located in the centre of the city, next to two of the emblematic religious buildings: the Cathedral and the "Basílica de la Virgen". To cover this underground museum, a public plaza, including a large square skylight of 17m sides (about 300 m^2), was erected.

As a result, greater sunlight is captured throughout the day and a transparency effect that draws the attention of the public, generating an open image. The skylight consists of a laminated glass plate with three sheets and on the upper part, there is a thin sheet of water, producing an undulating visual effect of the projected light [9]. The predominance of interior lighting is substantial, so much so that the general atmosphere of the museum depends entirely on the skylight, although it only covers 12% of the museum's roof.

The aesthetic result of the skylight has been praised by the public. But it is causing significant problems. Regular maintenance is required to clean and fix the appearance of leaks. This leads to condensation repairs or the drying effect that favours the formation of efflorescence [10] in the museum. In addition, it produces an increase in microorganisms, vegetation and insects, as well as low energy efficiency in the summer due to the greenhouse effect [11]. On the other hand, the great contrast of light between the illuminated areas under the skylight and the adjacent ones hidden by opaque roofing is unavoidable. Figure 1 shows photographs of the exterior and interior of the museum.

The aforementioned problems prompted initiatives by the authorities such as replacing the pond with a pyramidal skylight in the style of the Louvre in Paris [12], or eliminating the sheet of water [13], although this would make it difficult to control the temperature, according to Fernández-Navajas et al. [14] and Merello et al. [15]. For the moment, the situation remains intact [16].

In the review of previous works, conservation analyses of archaeology sites that are exposed to solar radiation are found. An excess of radiation was the trigger for the removal of the transparent protective structures of the Roman Palace of Fishbourne in West Sussex (England) and the Villa Romana of Piazza Armerina in

Citation: Juan-Carlos M, José Luis B; María-Antonia S; Fernando-Juan G-D. Statistical Analysis of Ultraviolet Radiation in The Museum of L'almoina in Valencia (Spain). Japan J Res. 2023;4(1):1-12

***Figure 1**. (a) Exterior of the "Museo de l'Almoina"; (b) interior of the museum just below the skylight.*

Sicily (Italy). In the work of Funda Yaka [17], the advantages and disadvantages of transparent protection are considered. For example, it is necessary to carefully select the material based on thermophysical properties. In other studies, it is recommended to combine lighting to visualize things and that it has little impact on the objects for their full conservation (see Michalsky [6,18,19]).

In other such works, for example, Horie [20], proposed the use of solar control films to reduce levels of sunlight without altering the internal and external appearance of the installation. The most widely used glass in museum skylights is laminated, which is why Al-Obaidi et al. [21] warned about the need to control UV rays, since, as several authors indicate [22–25], glass filters the UV-B band of solar radiation but transmits a large part of the UV-A band. Consequently, the type and thickness of glass used in the skylight have a great influence. Camuffo [5] comments on the simple physical effect that light absorbed in the form of heat affects the surface temperature and relative humidity can affect internal stress. This precise circumstance has been analysed inside the Museo de l'Almoina, measuring the conditions of humidity and temperature [14,15]

Tuchinda et al. [25] analysed the factors that affect the UV protection properties of glass. These properties include the type of glass, the colour, the intercalations and the coating. They found that clear glass allows up to 72% of UV light and up to 90% of VIS to pass through, depending on the thickness of the glass.

It has been studied that the transmittance in the VIS region of a quartz glass slab was greater than 78%, due to the absorption band, and between 40 and 80% in the UV-A region. The decrease in transmittance was also analysed as the thickness of the glazing sheets increased. Transmittance spectra were observed, detecting small differences between different film thicknesses in the VIS range (380–760 nm), and a large difference in the UV and NIR bands (see Li et al. [26]).

In the work of Serrano and Moreno [27], the spectral transmission of solar radiation by different translucent materials was analysed and, for smoked glass, they found transmittance values that range between 56 and 68% in the UV-B band and 70% in the UV-A band, with higher values in the VIS (85%) and NIR (80%) bands. For the smoked glass, lower transmittances were obtained at higher temperatures, and it likely has its origin in the reduction of the thermal conductivity when the temperature increases [28].

The performance of thermochromic double glazing in building application has been analysed [29], and the effect of double glazing specifically in a market [30].

In compliance with the preventive conservation of heritage proposed by the standard [31], the present work uses the term "relative attenuation" (RA) to the relationship between the external incident ray in a window and the maximum incident ray in an interior point, which it is not listed in the literature [32].

Mathematical studies have achieved great importance in archaeology. Certainly, it is an essential fact for the advancement of any discipline. In the research tasks of a specific objective, the mathematical methods constitute an abstract system of relationships, which help in the task of recognizing a registration scheme and specifying its nature. Of all the specialties of Mathematics, Statistics is the right one to try to bring order to the apparent confusion of the real world.

The present work complements the objective of analysing the spectral solar radiation that affects the interior of an archaeological museum through a skylight that contains a thin layer of water on top. In a previous article, the interest was to quantify the attenuation of solar radiation relative to the outside. Inside the museum, a series of points were chosen (north, south, east and central of the skylight) where the measurements were made, and given that their location is not directly after the incidence of sunlight (points north and east are under a roof), the concept that best fits when evaluating the decrease in intensity, is that of attenuation. The magnitudes that are most applicable are the relative ones, since they allow comparisons to be made between different sets of values, and even those obtained in other studies. Consequently, the internal measurement was relativized with respect to the external value, which is measured for each hourly series. Spectral measurements can report evolutions or disturbances in segments of the spectral bands. The global values provide an overview, but do not determine specific behaviours, and in the case of structures that partially block the light at certain measurement points, more information is obtained with the spectral radiation attenuated. And so much more, that it is possible to detect a pattern of behaviour of the museum structure, in the face of incident radiation. To reach this end, it has been decided to compare the interior values of the museum, with respect to a central interior value of the skylight that receives a maximum of solar radiation. In itself, there is a relationship of spectral attenuated radiation in each zone of the museum.

At the beginning of the study, an exploratory data analysis is carried out, placing greater emphasis on the visual representation of the data and not on exhaustive statistics derived from them. The basic idea is to explore the measures by dividing them into two components; the one that determines a general scheme and the component of disturbances with respect to the general scheme. Tukey (1980) [33] complements idea testing, calling it "confirmatory data analysis."

The visualization of the data is carried out by means of the distribution of frequencies (by tables) where a grouping of the observations in a limited number of categories has been previously established, in such a way that it is possible to distinguish whether the categories are expressed on a scale nominal, or if there is an inherent order in the bars.

Another aspect of interest in the analysis of experimental data is the association between distributions. In general, the studies focus on analysing the pattern shown by the distribution of a single type of physical magnitude. However, the factors that control and determine a model affect more than one distribution in a given work area. So, if you find out how the distributions are associated with each other, you get more information. In the case of the present work, the behaviour pattern of the data can be produced between the data distributions in the different positions and the winter and summer data. If the same factors affect two concurrent distributions or if there is an effect between them, their patterns will not be independent and the distributions will be positively or negatively associated. In statistics, to achieve this goal, the technique of "association tests and measures" is used. One method consists of the elaboration of the so-called contingency matrices, and the use of the χ^2 test using Croxton's formula (1953) [34], as duly explained in the Methodology section. Another more direct method is the use of "association degree indices", such as the "Q index" (or Yule index) (Gifford and Kroeber, 1937 [35]) (Kluckhohn, 1939 [36]), and the "V index" (Milke, 1935 [37]; Driver (1961 [38]). In this work we have chosen to use the Q index because its formula is simpler.

Solar radiation was measured in three bands: UV (300-400 nm), Visible (400-700 nm) and Near Infrared, depending on the interval (700-900 nm), (published in Serrano et al. [39]), and in this work the following tasks have been carried out: Analysis of UV values; evolution of the spectral radiation for each measurement point; the comparison between series of measurements (between interior points in the summer; and between summer and winter series), in order to contribute to the preventive conservation of the museum.

Materials and methods

Tested materials

The experimental measurements were carried out at the Museo de l'Almoina, in the historic centre of Valencia (Eastern Spain; 39º 28' N, 0º 22' W; at sea level). The element under study is a large skylight made up of laminated glass made up of 3 sheets of glass 10 mm thick joined together by sheets of polyvinyl butyral (PVB) (Figure 2). Such material has the task of increasing the flexural strength of the glass according to the adherence capacity of the sheets and guarantees safety against breakage. It also contributes to reducing the relative attenuation of UV radiation, as we verified in this study.

Spectral measuring devices

The relative attenuations were obtained from the measurement of the spectral irradiance outside and at different points inside

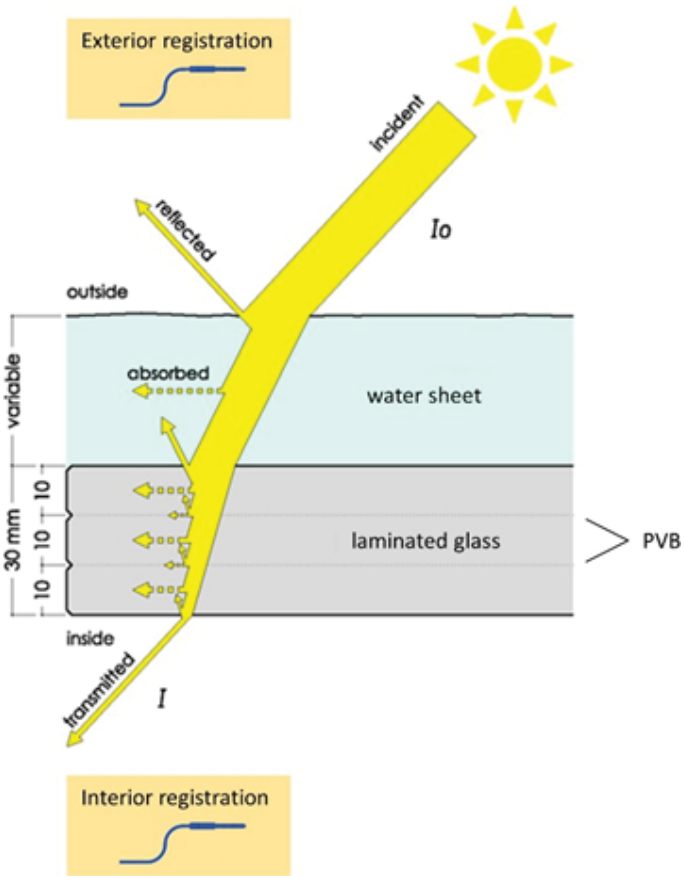

Figure 2. *Light intensity attenuation through the skylight the skylight and the water layer. The initial intensity is represented by "Io" so that it is reduced by the partial absorption and reflection that occurs circulating through the different layers, reaching the transmission of a fraction to the interior "I".*

Table 1. *Specifications of spectrometer used [42].*

Ocean Insight	FLAME-S-UV-VIS
Detector	Linear silicon CCD array
Entrance slit	25 µm
Grating	#1
Pixels	2048
Integration time	1 ms–65 s
Optical resolution	1.33 nm FWHM (typical)
Wavelength range	200–850 nm
Input fibre connector	SMA 905
Signal-to-noise ratio	250:1 (full signal)
Stray light	<0.10% at 435 nm
Calibration uncertainty	10%
Wavelength step	0.10 nm

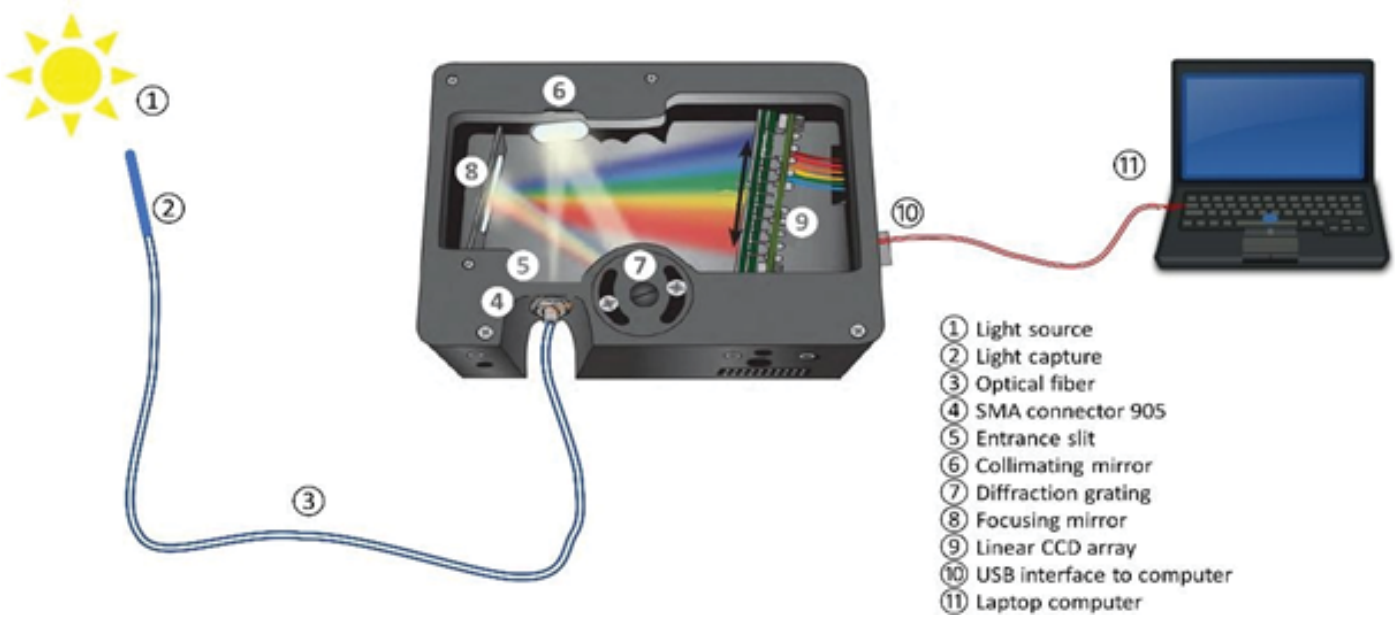

Figure 3. *Operating diagram of an optical spectrometer such as the one used in this study [41].*

were made using an Ocean Optics spectrometer [40]: FLAME-S-UV-VIS for the UV-B (280–315 nm) and UV-A (315–400 nm) bands.

The operation of this device is described in Figure 3, and technical specifications are shown in Table 1. The light is transmitted through a fibre optic cable and an SMA connector to the spectrometer. There is an entrance slit that regulates the amount of light incident on the optical bench and there is a regulating filter for the fixed wavelength region. Reflection of light occurs in the collimating mirror in the direction of the grating, producing diffraction. Subsequently, it is directed to the focusing mirror from which it is projected to the CCD (charge-coupled device) producing a conversion of the optical information into a digital signal. The transmission of the digital signal is made from the USB port to the computer for processing by the software.

The spectrometer was calibrated in July 2017 from 250 to 400, by Ocean Optics, with a measurement uncertainty of approximately 10% across the entire measurement spectrum.

As the UV-B radiation values below 300 nm with FLAME-S had a lot of background noise, they were discarded from the calculations. This range was organized into UV-B [300, 315] nm, and [315, 400] nm for UV-A.

Data collection

The capture and reception management of the information provided by the spectrometer was performed on a conventional PC using the SpectraSuite by Ocean Optics, suitable for FLAME-S-UV-VIS.

In the first place, outside the museum, the sensor was oriented towards the point of maximum light intensity that coincides with the solar position to record the normal spectral solar irradiance, and immediately afterwards the measurements of 4 points were made just below the projection of the skylight (Figure 4). Each measurement was performed twice in anticipation of possible errors. The points were "E" on the East, next to the landing of

Figure 4. *Spatial distribution of studied points. East point (E), Central point of the skylight (C), North point (N), and West point (W).*

the entrance stairs; point "N" on the North of the museum, on the corridor; "W" on de West side of the skylight; and point "C", on the central point under the skylight.

This procedure was repeated on different days throughout the year: one in winter (14 January 2020) and one in summer (30 July 2019). On both days, the skylight was filled with water, which is the usual situation except during maintenance and cleaning operations. The procedure was also repeated at different times of the day:

Table 2. *Solar zenith angle (SZA), in degrees, for the studied periods.*

	Morning	Noon	Afternoon
30/07/2019	44.84	19.94	41.80
14/01/2020	75.32	60.97	72.74

morning (9:00 AM), noon (12:00 PM) and afternoon (3:00 PM) (solar time). The two days when the spectral values were taken were clear. The solar zenith angle on the data collection days is shown in Table 2.

Calculation of relative attenuation

When light reaches a semi-transparent surface, part of it is reflected, part of it is absorbed and part of it is transmitted through the object (Figure 1). This phenomenon can be expressed by the following irradiance balance that can be particularized for each wavelength:

$$\text{Irrad}_{incident,\lambda} = \text{Irrad}_{reflected,\lambda} + \text{Irrad}_{absorbed,\lambda} + \text{Irrad}_{transmitted,\lambda} \quad (1)$$

Optical relative attenuation, as the main magnitude on which this entire study pivots, defines a relative (dimensionless) quantity that measures the fraction of incident light passing through a sample, in this case, the glass of the skylight. It is expressed by the result of dividing the transmitted light maximum intensity (I_{max}) by the incident maximum ray intensity ($I_{0,max}$).

The calculations for obtaining this relative attenuation values were based on the data provided by the spectrometer oriented to the maximum intensity of light (I_{max}, $I_{0,max}$) for each transmitted wavelength.

Comparative relative attenuations

$$RA = I_{max} / I_{0,max} \quad (2)$$

The relative attenuation calculations were compared at different times (9:00 AM, 12:00 PM and 3:00 PM solar hours) for the same season and same points to evaluate the influence of irradiance due to the different orientations and inclinations of the sun throughout the day.

The spectral values of all the points recorded by the UV-A and UV-B bands were considered for the same season, the same time and the same skylight situation (clear days without clouds) to take into account the spatial variations in relative attenuation inside the museum.

The selected data were arranged in tables and presented in graphs using Microsoft Office Excel for a clear visualization of the results.

Statistical study

In a first phase, the study of the data is merely descriptive. Statistics are used: mean, standard deviation and coefficient of variation, which facilitates the comparison of measures affected by different units. On the other hand, it facilitates the detection of data dispersion taking the central value as a reference. Another descriptive method is the representation of bar diagrams, which help to visualize the grouping of values at the different points in the museum, according to limited intervals. In this work, we are interested in determining the grouping of radiation attenuations within the interval [0 , 1], which corresponds at the unit end to a radiation equal to the central point C where the maximum luminosity falls.

As stated in the introduction, it is of interest to analyse the association between data distributions (in our case, the rounds of measurements made at the interior points of the skylight). In descriptive statistics, in general, the distribution of a single type of measurement, or batch of measurements, is studied. However, the factors that control and determine a pattern almost always affect more than one distribution. It is of great interest, therefore, to find out how the distributions are associated with each other, following the guidelines of the Analysis of Associations [35]. It consists first in the construction of the contingency matrix, which contains in the rows the frequencies of the values that are obtained in the arbitrary partition of the data. In this study, the interval [0 , 1] nm has already been mentioned; and the number of partitions of such interval is arbitrary, using [0 , 0.5] nm and [0.5001 , 1] nm. The proposed partition is placed both in a row and in a column, resulting in a square matrix (Table 3).

Table 3. *Contingency matrix for two variables.*

	DISTRIBUTION TYPE A	
DISTRIBUTION TYPE B	a	b
	c	d

The variables involved in this methodology correspond to the intervals of UV radiation attenuation at the points measured under the skylight.

The cells of the matrix represent a measure of the covariance of the distribution ranges of the values. Consequently, cell "a" means the joint presence of the values of the two distributions in the first range. Cell "b" means the joint presence of the values of the first range of distribution B and the values of the second range of distribution A. Similarly, cell "c" collects the presence of values in range two of distribution B with values in range one of distribution A. And finally, cell "d" is the covariation of the elements of the two distributions belonging to rank two.

The Q index is defined as,

$$Q = \frac{ad - bc}{ad + bc} \quad (3)$$

The interval of existence of the index is [-1 , +1], being the value (+1) the maximum positive association, and the value (-1) the maximum negative association, which corresponds to the segregation between distributions. The null value occurs when there is no evidence of association.

The values of the Q index are linked to the structure of the museum since the counting of the interdependent values (a, b, c, d of equation 3) depends directly on the shape of the premises.

Therefore, to generalize the results to different forms of buildings, the analysis extracts the information that the Q index can provide in general. That is, a specific index value implies frequencies appearance correlations of values ranges.

It is important to contrast causal association and inference. When an association between two distributions is detected, it does not necessarily infer a causal relationship. It should be investigated with other conditions, implying the introduction of other distributions. Since the originally selected Yule index represents a 2x2 matrix, when considering a third distribution, it will lead to a 2x2x2 contingency matrix (Table 4).

Table 4. *Contingency matrix for two variables.*

Ranks of z	Ranks of x and y	y	$\bar{y}$
z	x	a	b
	$\bar{x}$	c	d
$\bar{z}$	x	e	f
	$\bar{x}$	g	h

Being "x", "y", "z" three distributions, separated in two ranges. The letters "a" through "h", as in the definition of the Q index, are the intersections of the three distributions in the ranks.

First, the coefficient of order zero of the general table is determined [35]

$$Q_{xy} = \frac{[(a+e)(d+h)]-[(b+f)(c+g)]}{[(a+e)(d+h)]+[(b+f)(c+g)]} \quad (4)$$

Second, the partial coefficient is determined, controlling the "z" distribution,

$$Q_{xy/z} = \frac{(ad+eh)-(bc+fg)}{(ad+eh)+(bc+fg)} \quad (5)$$

Thirdly, both coefficients, zero and partial order, are compared, not registering changes when they are equal. It means that there are no differences in the relationships between "x" and "y" whether or not there is control over the third distribution. In other words, the third variable has no effect on the original bivariate relationship. In the case of detecting a lower value of the partial coefficient with respect to the zero order, it would imply that the relationship between "x" and "y" weakens when we control the third variable; that is, it is the variation of the third variable (or distribution) that explains the existence of the relationship between "x" and "y"

Results

Relative variations of the UV attenuation between interior points of the museum in summer

As detailed in the Methodology section, the radiation attenuations of three points inside the museum are compared. In a first phase, for a summer day, the relative variation of ultraviolet attenuation of the interior points is analysed, taking a central point of the skylight as a reference. The results are shown in Figures 5 to 8, where the spectral variations in the UV range are shown.

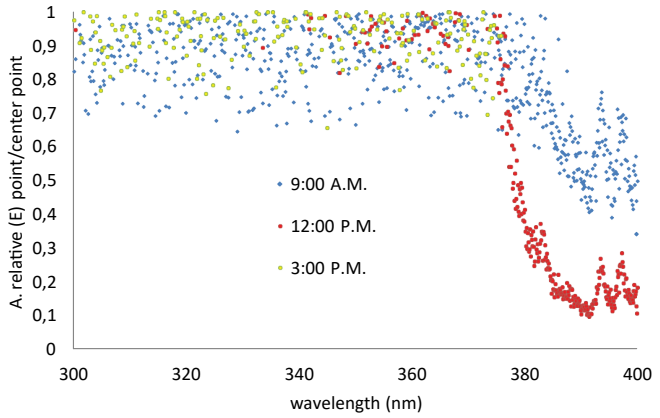

Figure 5. *Relative spectral variation between point E and point C in summer at different hours.*

In Figure 5, it can be observed that the range from 300 to 340 nm presents the same radiation at 3:00 PM at points C and E, decreasing this ratio towards the visible band (400 nm). This means that the central point C receives more UV radiation with respect to point E in the region of 380 to 400 nm. During the morning, a uniform behaviour is observed, implying an equalization of radiation between these points, producing a slight decrease in UV radiation in the area of 380 to 400 nm.

Calculated the averages of each series (Tables 5 to 7), it is obtained that, in summer, the E point in the mornings present an average of 0.79 less UV radiation, at midday 0.39 and in the afternoon 0.29 than C point. All this concerns the central point of the skylight. The entry point is located to the East with a view to the West. In such a way it captures less morning light, hence a lower average compared to the afternoon, which exerts greater luminosity. At noon, an average of less than three is found due to the exponential decay shown in Figure 5 The dispersion of the values is evaluated with the standard deviation, resulting in the afternoon series with the least dispersion (0.07) and the higher corresponds to the midday values (0.31). The coefficient of variation (standard deviation/average) of the three series is 0.20 for the morning, 0.80 at noon and 0.07 in the afternoon (Table 5).

Figure 6 shows that, throughout the day, the radiation in the UV-B and UV-A zones is uniform. Emphasizing that again at the end of 380 to 400 nm, there is more radiation in the central point.

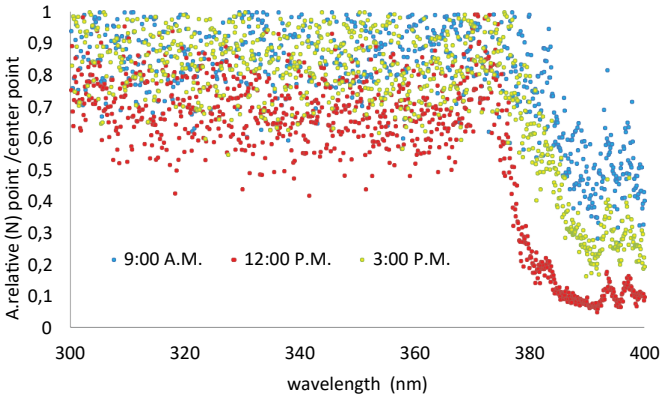

Figure 6. *Spectral relative variation between point N and point C of the skylight in summer.*

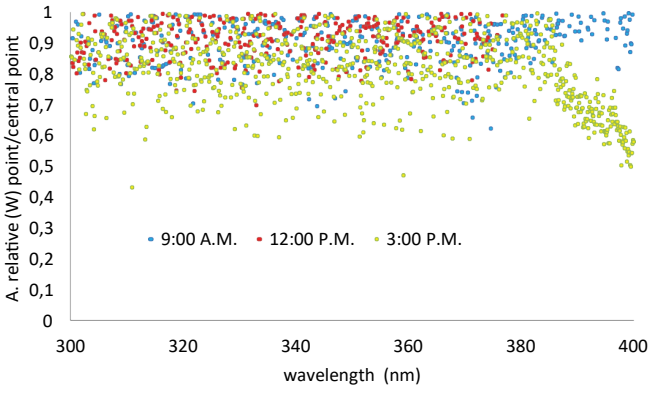

Figure 7. *Relative spectral variation between point W and point the C in summer.*

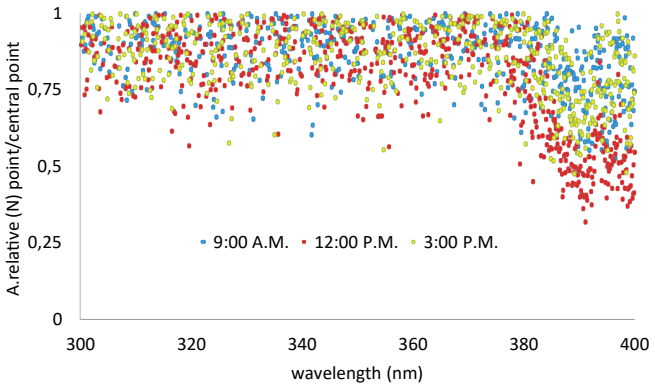

Figure 8. *Relative spectral variation between point E point and point C point in winter.*

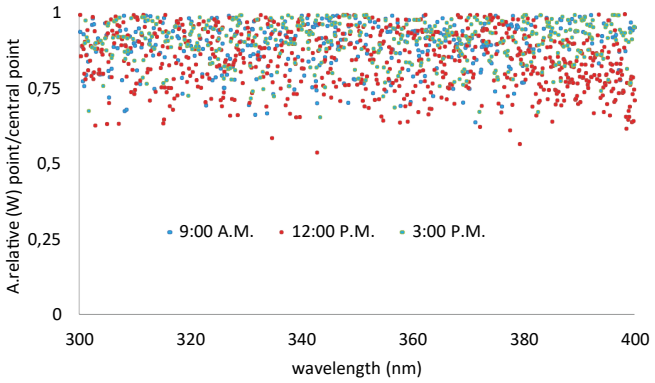

Figure 9. *Spectral relative variation between the N and C points of the skylight in winter.*

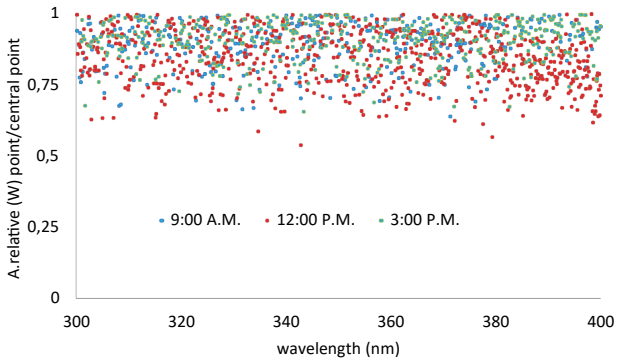

Figure 10. *Spectral relative variation between the W and C points of the skylight in winter.*

In the morning, at the North point, a slightly higher level of UV is detected throughout the spectral representation, and at noon, a slightly lower level of UV.

In Figure 6, the three series, a lower average level of UV radiation in summer of N point with respect C point are shown: 0.77; 0.56; 0.71, morning, noon and afternoon respectively. The standard deviations in the same order are: 0.17, 0.26 and 0.23, which leads to the coefficients of variation: 0.23, 0.46 and 0.32 (Table 6).

In Figure 7, throughout the day, the relative evolution of radiation is uniform except at the extreme of 380 to 400 nm, where at midday and in the morning, the average UV radiation is 0.9 and 0.91, respectively. And in the afternoon, it is an average of 0.81, with a higher standard deviation (0.11) and a higher coefficient of variation (0.13) being notable (Table 7).

Comparison of the relative radiation of UV radiation in summer and winter

Figure 8 shows the relative UV spectral variation between the East and Central points of the skylight. The uniformity of distribution of the points stands out in comparison with Figure 5. The greatest contribution to this effect is the lower inclination of the solar rays in their incidence in winter. This produces a greater share of diffuse radiation.

Figure 9 represents the relative spectral variation between point N and point C in winter and shows a similar variation to Figure 8. Compared with Figure 6, there is a less pronounced decrease near the visible region.

Figure 10 represents the relative UV variation between the W and C points. A complete uniformity of the point clouds is observed throughout the UV range. Distribution is very similar to Figure 7.

Next, some tables are indicated with the statistics, average, standard deviation, and coefficient of variation, of relative values of the previous summer and winter distributions.

The dispersion of the variations relative (Table 5) to noon are higher in summer, due to having more diffuse radiation.

In the morning (Table 5), a bias of the values less than unity is observed. A higher concentration of values is observed in the morning time slot.

The relative variation, being a radiation quotient, determines the radiation level measured at the central point, since its higher level leads to smaller attenuations. Table 5 shows that at noon and in the afternoon of summer, the radiation values are high and are similar at those times, since not only the level of radiation influences, but also the greater number of hours of insolation. In winter, on the contrary, the averages are higher due to a lower record of solar intensity in the central point due to the lower intensity and fewer hours of sunshine. This produces high relative variation ratios. Table 5 shows a high standard deviation at noon. This is a consequence of the multiple and intense reflections of radiation inside the museum, given the almost perpendicular incidence of external solar radiation. This effect causes an amplifying influence on the sensor, and therefore dispersion of the values.

The average of relative values between the N and C points (Table 6) is higher in winter for the same reason that there are higher diffuse radiation values and, as in Table 5, they produce greater dispersion. The participation of a higher percentage of diffuse radiation influences the measurement sensor. The north point is under a non-transparent ceiling and the sensor captures a higher diffuse component, and produces a uniformity of response at that point, therefore, the standard deviation row (figure 6) contains more constant values.

Between the N and C points (Table 6), it also shows a decreasing bias, which implies a lower level of radiation. For this case, it is recorded in the three series (schedules) of the day.

Table 5. *Comparison of statistics of the relative variations of UV between point E and point C in summer and winter.*

SUMMER			
	Morning	Noon	Afternoon
Average	0.79	0.39	0.29
Standard deviation	0.16	0.31	0.07
Coef. Variation	0.20	0.80	0.07
WINTER			
Average	0.85	0.79	0.86
Standard deviation	0.10	0.15	0.09
Coef. Variation	0.12	0.19	0.10

Table 6. *Comparison of statistics of the relative variations of UV between the N and C points of the skylight in summer and winter.*

SUMMER			
	Morning	Noon	Afternoon
Average	0.77	0.56	0.71
Standard deviation	0.20	0.26	0.23
Coef. Variation	0.23	0.46	0.32
WINTER			
Average	0.85	0.77	0.84
Standard deviation	0.10	0.17	0.11
Coef. Variation	0.12	0.22	0.14

Table 7. *Comparison of statistics of the relative variations of UV between the W and C points of the skylight in summer and winter*

SUMMER			
	Morning	Noon	Afternoon
Average	0.90	0.91	0.81
Standard deviation	0.07	0.06	0.11
Coef. Variation	0.08	0.07	0.13
WINTER			
Average	0.88	0.84	0.90
Standard deviation	0.08	0.09	0.07
Coef. Variation	0.09	0.11	0.08

The comparison in the case of relative radiation between the W and C points (Table 7) shows two important biases, namely: First, the afternoon series has a lower level of radiation at the W point in winter. In the summer and winter series, the attenuations at the north point are similar for the already mentioned reason of a higher level of diffuse solar radiation participation.

Analysis of association between distributions of measures

Between inland points in summer

All possible combinations between the measurement rounds were made by programming, that is, data attenuation at the C point (morning, noon, afternoon) with the E, N and W data. All of them, in turn, contain (morning, noon, afternoon), making a total of 36 calculations of the Q index. Of all the combinations, the most positive association (with a level between 30 and 40%) occurred between noon from the E point and the three series (morning, noon, afternoon) from the W point. The reason is that the W point is not under a roof and is opposite the E point in the skylight. The solar path incident so perpendicularly produces a partial equalization of illumination between these points, and therefore, a shared distribution to a certain degree.

The maximum negative association (between 75 and 100%) is exerted between the series of afternoon and morning of the E point with the same series of the W point. This means segregation between that data set, caused by the position of the Sun at those times and the shape of the skylight.

The association of distributions contributes to the knowledge of the behaviour pattern of the museum installation. One way to visualize it is through the graphical representation of the Q index

Table 8. *Q index between points E and N.*

		Point N		
		9:00 A.M.	**12:00 P.M.**	**3:00 P.M.**
Point E	**9:00 A.M.**	-0,5	-0,25	-0,81
	12:00 P.M.	0,21	0,09	0,14
	3:00 P.M.	-0,63	-0,15	-0,25

Table 9. *Q index between points E and W.*

		Point W		
		9:00 A.M.	**12:00 P.M.**	**3:00 P.M.**
Point E	**9:00 A.M.**	-0,73	-0,72	-0,80
	12:00 P.M.	0,34	0,33	0,39
	3:00 P.M.	-1,00	-1,00	-1,00

expressed as a function of the E and N points of the skylight. Alternatively, the same depending on the E and W points. Tables 8 and 9 show the result.

From Tables 8 and 9 it is deduced that the attenuation values between points E, N and W show a coevolution with positive association at midday, being more significant between points E and W, since they share greater illumination of the room at the central time of day, and this leads to an increase in the positive Q index of 60%, with respect to the Q index of points N and E. The reason for this difference is due to the shape of the skylight structure that has at point N a greater opaque roofing strip.

Table 9 shows that in the afternoon the coevolution of illumination, and therefore of attenuation, is very different between points W and E. There are more hours of insolation at point W, and this implies a very different coevolution in E and W, giving values of the Q index (-1).

The conclusion to be drawn from these tables is that the construction of the skylight gives rise to a coupling of the lighting values of the west and east sides, higher than those established between the east and north sides. The specific geometric characteristics of each building will produce different values of Q index.

This can be used to generalize the information. Indicating a Q value is associated with frequency correlations grouped into ranges that belong to different distributions. For example, the input distribution at morning in a specified range is compared to the distribution of a side point at the same time. This leads to a value of the contingency matrix.

To reinforce the association study between distributions (e. g. three distributions in summer (west, north and east) on a specific day in July at morning, equations (4) and (5) from the Methodology section are applied, obtaining an index value Qxy = -0.26, and as a partial index, Qxy/z = -0.245. In our case, the third distribution is the attenuation values at morning from the west point of the museum. So, by lowering the partial index a bit, you have a slight influence on the relationship between the north and east distributions of the museum. It is a logical result since the solar radiation in Valencia is very intense on the west side.

For another form of museum building, it will produce another value of the mentioned contingency table which, in turn, leads to the Q index. To evaluate hypothetical changes in increase or decrease of Q index, we proceed with the determination of the differential of equation (4); in this way, the variation of the Q index with respect to the values of the contingency matrix (a, b, c, d) is obtained. The parts of the differential of Q are:

$$\left(\frac{\partial Q}{\partial a}\right)_{b,c,d} = \frac{d[1-Q]}{ad + bc} \quad (6)$$

$$\left(\frac{\partial Q}{\partial b}\right)_{a,c,d} = \frac{-c[1+Q]}{ad + bc} \quad (7)$$

$$\left(\frac{\partial Q}{\partial c}\right)_{a,b,d} = \frac{-b[1+Q]}{ad + bc} \quad (8)$$

$$\left(\frac{\partial Q}{\partial d}\right)_{a,b,c} = \frac{-a[1-Q]}{ad + bc} \quad (9)$$

For example, in the comparison between point E and point N both in the morning, it has a result of Q = -0.5.

The contingency matrix is $\begin{pmatrix} 120 & 699 \\ 6491221 \end{pmatrix}$ the appropriate variations of Q with each element (equations from 6 to 9) provide the following values:

$$\left(\frac{\partial Q}{\partial a}\right)_{b,c,d} = 3{,}1 \cdot 10^{-3}\ ;\ \left(\frac{\partial Q}{\partial b}\right)_{a,c,d} = -6 \cdot 10^{-4}\ ;$$

$$\left(\frac{\partial Q}{\partial c}\right)_{a,b,d} = 5{,}3 \cdot 10^{-4}\ ;\ \left(\frac{\partial Q}{\partial d}\right)_{a,b,c} = -3 \cdot 10^{-4}$$

It is noteworthy that the rate of change of the index against the elements of the contingency matrix is greater in the element of the first row and first column. Accounting for the frequencies in the low range [0, 0.5] nm of both the entry point and lateral distributions in the morning.

If we assume a different skylight structure, it will imply modification of the elements of the contingency matrix (that is, coincidence of frequency of values grouped in ranges, of two hourly distributions). Assume the following element modification: a = 5; b = 0; c = 0; d = -5; means that it increases the frequency of values in small ranges and decreases the frequency in large ranges. So, the variation of Q leads to the value, dQ = 0.018; such that the final result of the index will be, Q + dQ = -0.5 + 0.018 = -0.482.

So far, information on the distribution of values association is available; its modification due to changes in the shape of the skylight, and by means of equations (6 to 9) the rates of change of the index are obtained against the variations of the elements of the contingency matrix.

Between points in different seasons (summer and winter)

The association of the points at the same time in winter and summer has been studied. The results are: West point (summer-winter comparison), Q = -1. It means negative association (mutual segregation of values). North point, Q = -0.40. The E point, in the morning and afternoon strongly negative, and positive with Q = 0.30 in the comparison of the E point at noon, in the summer and winter rounds. This last result implies an orientation characteristic of the museum that allows a slight coupling of the values between opposite stations.

The variation of the Q index, in the comparison of the W point (summer-winter) leads to the following results: rates of variation of the elements of the contingency matrix.

$$(\frac{\partial Q}{\partial a})_{b,c,d} = 1,52\cdot10^{-2};\ (\frac{\partial Q}{\partial b})_{a,c,d} = -4\cdot10^{-3}$$

$$(\frac{\partial Q}{\partial a})_{a,b,d} = -1,11\cdot10^{-2};\ (\frac{\partial Q}{\partial b})_{a,b,}c = 0$$

Higher rates of change in the comparison between seasons, than in the previous case, the comparison of two points in the same season of the year. Continuing with the proposed differentials: a = 5; b = 0; c = 0; d = -5, an index differential is obtained, dQ = 0.131, resulting in a final index, Q + dQ = -0.5 + 0.018 = -0.369.

The rates of change of the Q index are higher when changing values in the lower attenuation intervals (see table 3 and comments). It follows those lower attenuations in value have a greater influence of the shape of the museum building.

Discussion

The relative spectral variation between the west point and the central point of the skylight in summer, is uniform except at the extreme of 380 to 400 nm, where at noon and in the morning, the average UV radiation is 0.91 and 0.90, respectively. And in the afternoon, it is an average of 0.81, with a higher standard deviation (0.11) and a higher coefficient of variation (0.13) being notable.

The dispersion of the variations relative to noon are higher in summer, due to having more diffuse radiation.

In the morning, a bias of the values less than unity is observed. A higher concentration of values is observed in the morning time slot. It is significant that in the afternoon the opposite happens, the radiation is higher than in the central point.

The analysis of association between distributions of measures of the same summer leads at the maximum negative association (between 75 and 100%) is exerted between the series of afternoon and morning of point E with the same series of point W. This means segregation between that data set, caused by the position of the Sun at those times and the shape of the skylight.

The association of distributions contributes to the knowledge of the behaviour pattern of the museum installation. One way to visualize is through the graphical representation of the Q index expressed as a function of points E and N of the skylight. Alternatively, the same depending on the E and W points.

Then the changes in the structure of the museum building mostly affect the comparative results between the summer and winter seasons.

In summary, the study of the behaviour of the skylight under solar radiation has been focused on spectral study, providing a difference in attenuations at different times of the day, especially in the UV-A zone.

The comparison of relative radiation in summer and winter of points W and C (Table 7) shows two differences. First, the afternoon series has a lower level of radiation at point W in winter. Second, the morning and noon series have higher radiation than point C.

Notions of spatial statistics have been applied, since an architectural structure has geometrical characteristics that translate into a specific behaviour in front of external influences, such as solar radiation. Therefore, it is important to parameterize this behaviour, which will be useful in terms of predictions and comparisons between structures.

The authors' interest in following works is to carry out a spectral spatial parametrization (index Q) of this museum of l'Almoina. It will undoubtedly help to better understand and predict the possible effects of solar radiation on cultural heritage.

Author contributions

J.-C.M.E., conceptualization, methodology, formal analysis, writing—original draft, preparation, writing—review and editing. M.-A.S., conceptualization, methodology, formal analysis, writing—original draft, preparation, writing—review and editing. J.-L.B.Z., formal analysis, writing— original draft, preparation, writing—review and editing. F.-J.G.-D., formal analysis, preparation, writing— review and editing, funding acquisition. All authors have read and agreed to the published version of the manuscript.

Funding

This research was funded by the European Union's Horizon 2020 research and innovation program under grant agreement No. 814624.

Institutional review board statement

Not applicable

Informed consent statement

Not applicable.

Author contributions

The authors are grateful to the "Ajuntament de València" and to Vicent Escrivà Torres, director of the "l'Almoina" museum, for their assistance and authorization of the data collection to carry out this work.

Conflicts of interest

The authors declare no conflict of interest. The funders had no role in the design of the study; in the collection, analyses, or interpretation of data; in the writing of the manuscript, or in the decision to publish the results.

References

1. Committee for drafting the International Charter for the Conservation and Restoration of Monuments. International Charter for the conservation and restoration of monuments and sites (The Venice Charter). In 2nd International Congress of Architects and Technicians of Historic Monuments, 1964; art. 14.
2. International Committee for the Management of Archaeological Heritage (ICAHM). Charter for the Protection and Management of the Archaeological Heritage (Icomos Charter); 1990; art. 6.
3. Commission Internationale de L'éclairage. Control of Damage to Museum Objects by Optical Radiation; Fer: Vienna, Austria, CIE 157:2004 Division 3 ISBN: 9783901906275
4. Conservación del Patrimonio Cultural. Especificaciones para el Emplazamiento, Construcción y Modificación de Edificios o Salas Destinadas al Almacenamiento o Utilización de Colecciones del Patrimonio. UNE-EN 16893:2019. Asociación Española de Normalización (UNE), Madrid; 2019.
5. Camuffo D. Chapter 4. Radiation and Light. Conservation, Restoration, and Maintenance of Indoor and Outdoor Monuments. In Microclimate for Cultural Heritage; Elsevier: Amsterdam, The Netherlands, 2014; pp. 131–164.
6. Michalski, S. Light, ultraviolet and infrared. In Agent of Deterioration: Light, Ultraviolet and Infrared; Available online: https://www.canada.ca/en/conservation- institute/services/agents-deterioration/light.html (accessed on 08 April 2022).
7. Ribera, A. El centro Arqueológico de l'Almoina. Valencia. In Proceedings of the 5. Encuentro Internacional. Actualidad en Museografía, Palencia, Spain, 1-3 Octuber 2009; pp. 67–82.
8. Ribera i Lacomba, A. El centro arqueológico de l'Almoina en Valencia. In Archeologia e Città: Riflessione Sulla Varizzazione dei Siti archeologici in Aree Urbane; Ministero dei Beni e delle Attività Culturali e del Turismo. Soprintendenza Speciale per i Beni Archeologici di Roma, Palombi editore; 2012; pp. 37-45.
9. Herrera García JM, Rueda Muñoz de San Pedro JM. Memoria del "Proyecto de Ejecución para las Obras de Cimentación, Estructura y Cubierta Mediante Plaza Pública de los Restos Arqueológicos de l'Almoina de Valencia; Unpublished; 2002. Available online: https://dogv.gva.es/datos/2001/11/29/pdf/2001_M11450.pdf (accessed on 08 April 2022).
10. Pérez Ema N. Degradación del material pétreo en yacimientos arqueológicos. Rev. electrónica ReCoPar. 2016;11:39–58.
11. Padfield T. How to Keep for a While What You Want to Keep forever; Available online: https://www.conservationphysics.org/phdk/phdk_tp.html (accessed on 08 April 2022).
12. García H. El Estanque de la Plaza de la Almoina se Sustituirá por un Lucernario Piramidal; Available online: https://www.levante- emv.com/valencia/2013/05/19/estanque-plaza-almoina-sustituira-lucernario- 12896876.html (accessed on 08 April 2022).
13. Moreno P. El Centro Arqueológico de la Almoina de Valencia se Reformará a los once Años de su Apertura. Available online: https://www.lasprovincias.es/valencia- ciudad/ayuntamiento-encarga-estudio-almoina-20181024131618-nt.html (accessed on 08 April 2022).
14. Fernández-Navajas Á, Merello P, Beltrán P, García-Diego F. Multivariate thermo-hygrometric characterisation of the archaeological site of Plaza de l'Almoina (Valencia, Spain) for preventive conservation. Sensors. 2013;13:9729–9746.
15. Merello P, Fernández Navajas Á, Curiel-Esparza J, Zarzo M, García-Diego
16. FJ. Characterisation of thermo-hygrometric conditions of an archaeological site affected by unlike boundary weather conditions. Build Environ. 2014;76:125–133.
17. García H. Descartan la Pirámide de Cristal de la Almoina por el Efecto Sauna en el Museo. Available online: https://www.levante- emv.com/valencia/2013/06/05/descartan-piramide-cristal-almoina-efecto- 12891562.html (accessed on 08 April 2022).
18. Çetin FY, İpekoğlu B. Impact of transparency in the design of protective structures for conservation of archaeological remains. J Cult Herit. 2013;14:e21– e24.
19. Michalski S. Damage to museum objects by visible radiation (Light) and ultraviolet radiation (UV). In Proceedings of the Lighting in Museums, Galleries and Historic Houses, Bristol, UK, 9–10 April 1987; Papers of the Conference; pp. 3–16.
20. Michalski S. The Lighting Decision. In Fabric of an Exhibition, Preprints of Textile Symposium 97; Canadian Conservation Institute: Ottawa, ON, Canada, 1997, pp. 97-104.
21. Horie CV. Solar control films for reducing light levels in buildings with daylight. Stud Conserv. 1980;25:49–54.
22. Al-Obaidi KM, Ismail M, Abdul Rahman AM. A review of skylight glazing materials in architectural designs for a better indoor environment. Mod Appl Sci. 2014;8:68.
23. Parisi A. Quantitative evaluation of the personal erythemal ultraviolet exposure in a car. Photodermatol Photoimmunol Photomed. 1998;14:12–16.
24. Kimlin MG, Parisi A. Ultraviolet radiation penetrating vehicle glass: A field based comparative study. Phys Med Biol. 1999;44:917–926.
25. Kimlin MG, Parisi A, Carter B, Turnbull D. Comparison of the solar spectral ultraviolet irradiance in motor vehicles with windows in an open and closed position. Int J Biometeorol. 2002;46:150–156.
26. Tuchinda C, Srivannaboon S, Lim HW. Photoprotection by window glass, automobile glass, and sunglasses. J Am Acad Dermatol. 2006;54:845–854.
27. Li D, Li Z, Zheng Y, Liu C, Lu L. Optical performance of single and double glazing units in the wavelength 337–900 nm. Sol. Energy. 2015;122:1091–1099.
28. Serrano MA, Moreno JC. Spectral transmission of solar radiation by plastic and glass materials. J Photochem Photobiol B Biol. 2020;208:111894.
29. Fernández-Rojas F, Fernández-Rojas C, Salas KJ, García VJ, Marinero E. Conductividad térmica en metales, semiconductores, dieléctricos y materiales amorfos. Rev Fac Ing UCV Caracas. 2008;23:5–15.
30. Long L, Ye H, Zhang H, Gao Y. Performance demonstration and simulation of thermochromic double glazing in building applications. Sol Energy. 2015;120:55–64,
31. Aguilar JO, Xamán J, Olazo-Gómez Y, Hernández-López I, Becerra G, Jaramillo OA. Thermal performance of a room with a double glazing window using glazing available in Mexican market. Appl Therm Eng. 2017;119:505–515.
32. International Commission on illumination CIE DIS 017/E:2016 ILV: International Lighting Vocabulary. Available online: https://cie.co.at/e-ilv (accessed on 08 April 2022).
33. CEN/TS 16163:2014 Conservation of Cultural Heritage. Guidelines and Procedures for Choosing Appropriate Lighting for Indoor Exhibitions. Available online: https://standards.cen.eu/dyn/www/f?p=204:110:0::::FSP_PROJECT:34047&cs=1AFCAEA358660F36ECF4D92D51A8AD2FC (accessed on 08 April 2022).
34. Tukey JW. We need both exploratory an confirmatory. American Statistician. 1890;34:23-35.
35. Croxton FE. Elementary statistics with applications in medicine

and the biological sciences. Dover Pubns. 1953.
36. Gifford EW, Kroeber AL. Culture element distributions: IV, Pomo. University of California. Publications in American Archaeology and Ethnology. 1937;37:117-255.
37. Kluckhohn C. On certain recent applications of association coefficients to ethnological data. American Anthropologist. 1939;41:345-377.
38. Milke W. Sudostmelanesien, eine ethnostatistiche Analyse. Wurzburgo. 1935.
39. Driver HE. Introduction to statistics for comparative research. Publicado en Moore, F.W. ed. Readings in cross-cultural methodology. Hraf Press, New Haven, 1961. pp. 303-331.
40. Serrano MA, Baró Zarzo JL, Moreno Esteve JC, García-Diego FJ. Spectral Relative Attenuation of Solar Radiation through a Skylight Focused on Preventive Conservation: Museo de L'almoina in Valencia (Spain) Case Study. Sensors. 2021;21:4651.
41. Ocean Optics, Spectrometers. Available online: https://www.oceaninsight.com/products/spectrometers/ (accessed on 29 July 2021).
42. Reworked from Ocean's diagram. Available online: https://www.oceaninsight.com/products/spectrometers/ (accessed on 29 July 2021).
43. Ocean Insight. Available online: https://www.oceaninsight.com/products/spectrometers/ (accessed on 29 July 2021).